Kinetics of steam-char reaction of olive residues

Mauro Prestipino
Department of Engineering
University of Messina (*Italy*)
email: mprestipino@unime.it

Abstract—**Steam gasification is a thermochemical process that is suitable for efficient biomass conversion for stationary power production, especially in small scale applications. Steam-char reaction result to be the one of the most relevant and controlling step of the gasification process, hence a fundamental understanding of the kinetics of this heterogeneous reaction is needed in the design of efficient gasification systems. In this work, the reaction kinetics of char derived from olive pomace and steam was investigated. The kinetic study was developed by means of thermogravimetric analysis carried out in steam-nitrogen atmosphere, using an integral isoconversional approach. The ultimate and proximate analysis of the parent biomass was determined, while the char morphology was studied through scanning electron microscopy and nitrogen isothermal adsorption analysis for determining the specific surface area. The morphological analysis were carried out on the pristine char and the char after 50% of conversion in nitrogen-steam atmosphere. The results of the kinetic study showed slight variation of activation energy with conversion, with an average value of 161 kJ/mol. The reaction order showed an average value of 0.94, with negligible variation during conversion.**

Index Terms—**Syngas, Biomass, Kinetics of steam-char reaction.**

I. INTRODUCTION

The need of renewable sources of energy and materials is one of the main concerns of global community for a sustainable future development [1], [2], [3]. Biomass is considered as a promising renewable source of raw materials and fuels, because it is predictable, globally spread and it can be replaced faster than fossil raw materials, which take different centuries to be formed. Because of its rapid growth, biomass is able to store and release carbon, when burned, in a short time if compared to what happened for fossil fuels [4], [5], [6]. For this reason biomass derived fuels are considered carbon neutral. It is trivial to state that sustainable supply chain of bio-sources needs to be set up, in order to consider biofuels as really sustainable energy sources [7], [8], [9]. The use of residual biomass or wastes leads to further economic and environmental advantages, because it is possible to solve the problems related to its management and correct disposal [10], [11], [12], [13]. As substitute of fossil fuels, biomass can be exploited through different technologies, depending on the raw bio-material and on the final application [14], [15], [16], [17]. From lignocellulosic biomass, it is possible to produce liquid, gaseous or solid fuels [18], [19], [20]. Among the different thermochemical technologies, gasification is one of the most suitable pathway for sustainable on-site stationary
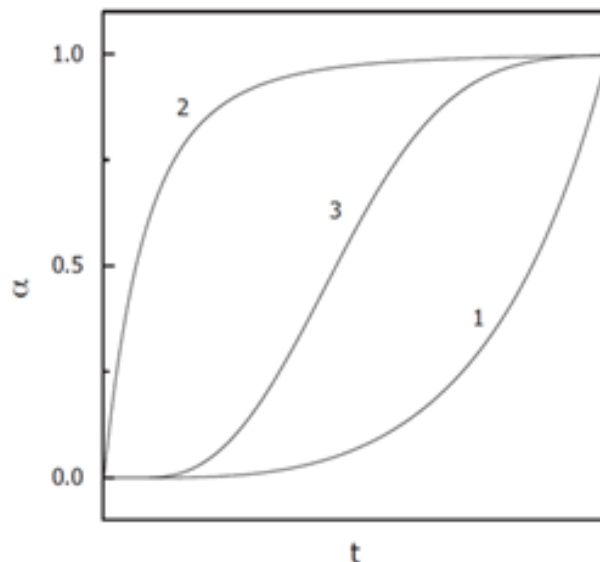
Fig. 1. α vs t reaction profiles for (1) accelerating, (2) decelerating, (3) sigmoidal models.

power production. Indeed, it is possible to use the producer gas (syngas) in internal combustion engines, gas turbines, fuel cells, or gas boilers [21], [22]. Another application of syngas is liquid fuel production through the Fischer-Tropsch process [23], [24], [18]. The most common configuration of biomass gasification systems are air-fed gasifiers [25], [19]. However, air-steam gasification leads to higher efficiencies and allows to produce a hydrogen rich syngas [25], [26], [27].

In thermal gasification systems, the lignocellulosic biomass undergoes drying, devolatilization and char gasification [28], [29]. The latter is one of the slowest thermochemical step and a fundamental understanding of the heterogeneous reaction kinetics is needed in the design of efficient gasification systems. When steam is used as gasification medium, steam-char reaction is the most relevant and controlling step of the gasification process [30], [31], [32], [33]. There are several reaction models that can properly describe the kinetic behavior of a material conversion process [34], [35], [36]. All the reaction models can be grouped in three major classes, according to the reaction profile of α vs t (Fig. 1): accelerating, decelerating and sigmoidal models [37], [38].

Accelerating models describe processes whose reaction rate increases with conversion (curve 1), reaching the maximum at the end of conversion process. This type of models are usually

TABLE I.   Reaction Models Used to Described Thermal Decomposition in Solids

Reaction model	$f(\alpha)$	$g(\alpha)$
Power law	$4\alpha^{3/4}$	$\alpha^{1/4}$
Power law	$3\alpha^{2/3}$	$\alpha^{1/3}$
Power law	$2\alpha^{1/2}$	$\alpha^{1/2}$
Power law	$2/3\alpha^{-1/2}$	$\alpha^{3/2}$
One-dimensional diffusion	$1/2\alpha^{-1}$	α^2
Mampel (first-order)	$1-\alpha$	$-\ln(1-\alpha)$
Avrami-Erofeev	$4(1-\alpha)[-\ln(1-\alpha)]^{3/4}$	$[-\ln(1-\alpha)]^{1/4}$
Avrami-Erofeev	$3(1-\alpha)[-\ln(1-\alpha)]^{2/3}$	$[-\ln(1-\alpha)]^{1/3}$
Avrami-Erofeev	$2(1-\alpha)[-\ln(1-\alpha)]^{1/2}$	$[-\ln(1-\alpha)]^{1/2}$
Three-dimensional diffusion	$2(1-\alpha)^{2/3}(1-(1-\alpha)^{1/3})^{-1}$	$[1-(1-\alpha)^{1/3}]^2$
Contracting sphere	$3(1-\alpha)^{2/3}$	$1-(1-\alpha)^{1/3}$
Contracting cylinder	$2(1-\alpha)^{1/2}$	$1-(1-\alpha)^{1/2}$
Second-order	$(1-\alpha)^2$	$(1-\alpha)^{-1}-1$

described by a power-law model:

$$f(\alpha) = m\alpha^{\frac{(m-1)}{m}} \tag{1}$$

The decelerating models represent reactions whose conversion rate reaches the maximum at the beginning of the process and it decelerates continuously, according to the common expression:

$$f(\alpha) = (1-\alpha)^m \tag{2}$$

The reaction models belonging to the sigmoidal group represent process that are composed by the combination of both accelerating and decelerating processes at the initial and final stages, respectively. The Avrami-Erofeev models typically represent the sigmoidal kinetic behavior:

$$f(\alpha) = m(1-\alpha)[-ln(1-\alpha)]^{\frac{(m-1)}{m}} \tag{3}$$

The most relevant reaction models are listed in the following Table I, in which it is also possible to find the integral form of the conversion model, $g(\alpha)$. However, the determination of the exact reaction model involves several iterative calculation. Furthermore, the application of model-fitting methods aims at determining one single kinetic value of the overall process, obtaining an average value These drawbacks can be avoided through the application of iso-conversional methods, which allow determining the kinetic parameters as function of conversion, without making any assumption about the exact reaction model. From the above, this work aims at investigating the gasification kinetics of chars obtained from agro-industrial wastes, in an atmosphere consisting of steam and nitrogen. The kinetic study was conducted by means of isothermal thermogravimetric analysis through an isoconversional method. The thermogravimetric study was accompanied by the char by the morphological and compositional characterization of biomass and char.

II. Materials and Methods

In this study, the char of olive residues is investigated. The char was obtained through the pyrolysis of dried olive pomace (OP) from olive oil production process.

### A. Material Characterization

Proximate and ultimate analysis of OP were carried out through a thermogravimetric analyzer (Netzsch 449ST Jupiter F3) and a CHNS/O analyzer (Perkin Elmer CHNS/O), respectively. After the biomass characterization, the dried sample was subjected to pyrolysis in a tubular quartz reactor at 500° C in nitrogen atmosphere for 1 h, in order to obtain the char. The inorganics in char sample were analyzed by an inductively coupled plasma-optical emission spectroscopy (ICP-OES).

Morphological characterizations of chars were performed by mean of a scanning electron microscope (SEM) and gas adsorption isotherms, then followed by the BET (BrunauerEmmettTeller) analysis for calculating the specific surface area. The morphological analysis were carried out on the pristine char and the char after 50% of conversion in steam-nitrogen atmosphere.

B. Thermogravimetric Analysis and Theoretical Approach

The kinetic study of the heterogeneous reactions were performed by means of thermogravimetric analysis in steam-nitrogen atmosphere and at isothermal conditions. The selected temperature range for the isothermal runs were below 800° C in order to guarantee as much as possible kinetics controlled conditions. In particular, the temperature range of 650-750° C was investigated, with steps of 25° C, and in a steam partial pressure of 50.6 kPa. The effect of steam partial pressure on chars gasification reactions was evaluated at isothermal conditions (700° C) and varying the gasifying medium (steam) partial pressure from 10.1 to 50.6 kPa, using nitrogen as complement. The TG apparatus consists in a vertical and cylindrical reactor that can be heated up to the desired temperature at different reactive atmospheres. The sample is kept in an inert area at room temperature on the top of the apparatus, and then lowered down in the reactor when the desired conditions are reached, in order to perform the tests at isothermal conditions. The thermogravimetric apparatus consists also in a steam generator kept at 250° C, as well as the transfer line, in which the water was fed by a HPLC pump. About 60 mg of char, with particle size $\leq 200\mu m$, was loaded in a cylindrical sample holder.

The apparent activation energy (Ea) and the reaction order (n) where determined by means of an isoconversional approach. This method allows determining the kinetic parameters as a function of the extent of conversion without making any assumption about the reaction model. For this reason, it is also known as model-free method. In particular, the integral version of the isoconversional approach was used, because it is not sensitive to noise in the experimental data, that is intrinsic to the experimental set-up system, since the experimental apparatus gives only TGA data (i.e. integral) as output result. The global reaction of char decomposition in steam gasification conditions that was considered in this work can be written as:

$$C + H_2O \leftrightarrow CO + H_2 \tag{4}$$

63
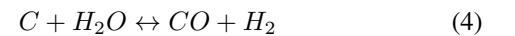
A typical equation describing a kinetic process can be expressed as follow:

$$\frac{d\alpha}{dt} = Ae^{(-\frac{E_a}{RT})}P^n H_2 O f(\alpha) \quad (5)$$

where f() is the reaction model, n is the reaction order with respect to steam, PH2O is the steam partial pressure, expressed in kPa, R [J/Kmol] is the gas constant, A is the pre-exponential factor, and is the char conversion, that is expressed according to the following equation:

$$\alpha = \frac{m_i - m_t}{m_i - m_f} \quad (6)$$

where m_i, m_t and m_f are the initial mass, the mass at time t and the final mass, respectively. From the integration of eq. 2, the following is obtained:

$$ln\, t_{\alpha,i} = ln\, \frac{g(\alpha)}{P_{H_2O}^n A} + \frac{E_a}{RT_i} \quad (7)$$

where:

$$g(\alpha) = \int_0^\alpha \frac{d\alpha}{f(\alpha)} = \int_0^t exp(\frac{-E_a}{RT})dt \quad (8)$$

by rearranging and integrating eq. 5, it is also possible to obtain the linear correlation between the steam partial pressure the logarithm of conversion time. This leads to eq. 6, from which the reaction order can be obtained by plotting $ln\, t_{\alpha,i}\, vs\, ln(P_{H_2O})$. The slope of the resulting straight lines represent:

$$ln\, t_{\alpha,i} = ln\left[\frac{g(\alpha)}{A} + \frac{E_a}{RT}\right] + nln(P_{H_2O}) \quad (9)$$

E_a is the apparent activation energy (kJ/mol) obtained at a specific value of conversion, which can be evaluated from the slope of ln t vs T^{-1}. Despite the pre-exponential factor is included in the term of the reaction model, it is possible to obtain its values at different degrees of conversion through the application of the compensation effect. This is based on the consideration that activation energy and pre-exponential factor are always linked by the following relationship:

$$ln\, A_j = \alpha E_j + b \quad (10)$$

a and b are coefficients that can be obtained by applying different reaction models which allow to obtain different A_j and E_j values at j-th reaction model. According to this approach, it is not necessary to find the exact reaction model, but the reaction models that are able to give back a linear correlation between $g(\alpha)$ and t, as reported by the following equation, which is obtained by integrating and rearranging eq. 5:

$$g_j(\alpha) = k_j(T_i, P)t \quad (11)$$

Where the subscript j indicates the various reaction models. Once that the rate constant in eq. 11 is determined, from its the logarithm expression is it possible to calculate the activation energy and the pre-exponential factor for the j-th model. Appling different reaction model, with this method is possible to calculate the a and b coefficients. Then, the isoconversional activation energy values can substituted in eq. 10 in order to calculate the isoconversional pre-exponential factor at different values of conversion. With such approach, the kinetics triplet can be obtained using a model-free method.

III. RESULTS AND DISCUSSION

A. Biomass and Char Characterization

The ultimate and proximate analysis are shown in table II, expressed in dry basis (db) and semidry basis (sdb), respectively. The high carbon content makes this material suitable for energy conversion, while the high volatile matter (VM) fraction confirms its good attitude to be converted through gasification processes.

The inorganic composition of the olive pomace char was determined because of the influence of the metal components on the kinetic of char conversion in presence of steam (see table III). Indeed, it is known the inhibiting effects of Si and P, and the catalytic effect of K on the steam-reaction.

From table III it is possible to notice that the high concentration of silicon is well compensated by potassium, which has the role to accelerate the reaction. Results of scanning electron microscopy are shown in Fig. 2 and Fig. 3. The
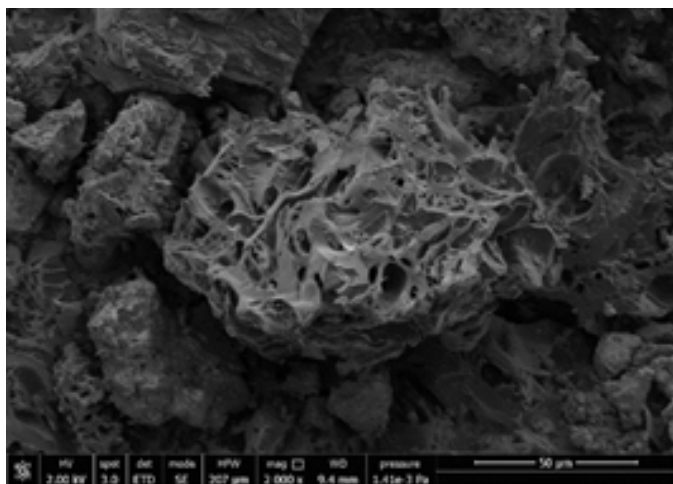
TABLE II. ULTIMATE AND PROXIMATE ANALYSIS OF OLIVE POMACE BY DIFFERENCE

Ultimate Analysis (%wt$_{db}$)					
C	H	N	S	O^a	Ash
52.1	6.4	1.2	0.1	36.1	4.1
Proximate Analysis (%wt$_{sdb}$)			
VM	FC	Ash	Moisture
70.2	23.8	4.0	2.0

TABLE III. INORGANIC COMPOSITION OF OLIVE POMACE CHAR

Element	Value [g/kg]
K	23.87
Ca	8.62
Fe	1.43
Na	0.62
Mg	1.50
Al	1.57
Si	9.23
P	1.35

Fig. 2.   SEM images of olive pomace char at 0%.

Fig. 3.   SEM images of olive pomace char and 50% of conversion.

SEM images were obtained for char at 0% (Fig. 2) and 50% of conversion (Fig. 3) under steam atmosphere. It is evident the heterogeneous structure of chars, especially before the steam-char reaction started. At 50% of conversion it can be noticed the formation of bigger pores in the external surface of the material. The char's morphology was further investigated through the BET analysis for the surface area calculation. This analysis revealed that the char has a low surface area, related to its microporosity, before the steam gasification process, showing values about $4\,m^2/g$. At 50% of conversion in steam atmosphere, a significant increase of the BET surface area was observed, reaching up to $500\,m^2/g$. This implies the formation of a micro-structured network, which is accompanied by the formation of large openings on the external surface, as evidenced by the SEM images.

B. Isothermal Thermogravimetric Analysis

The first approach for handling the thermogravimetric data consisted in plotting the extent of conversion as function of time, as reported in Fig. 4. From this graph it is possible to have a quick information about the reactivity of the analyzed sample. In fact, the shorter is the time to reach a specific degree of conversion, the higher is the reactivity. Furthermore, the shape of vs time plot gives important information about the mechanism of reaction. It is possible to notice that this sample shows a sigmoidal conversion mode, showing both accelerating and decelerating behaviors, reaching the maximum of the reaction rate at an intermediate value of conversion. This reaction profile can be associated to the Avrami-Erofeev models. From Fig. 4 it is also possible to observe how the time needed to reach a certain value of conversion is highly influenced by the temperature increase for temperatures lower than 700° C. Indeed, when the temperature is increased from 650° C to 675° C, the time that is necessary to reach 90% of conversion decreases from 5500s to 2950s, while it is 1500s, 1138s and 770s at 700, 725 and 750° C, respectively.
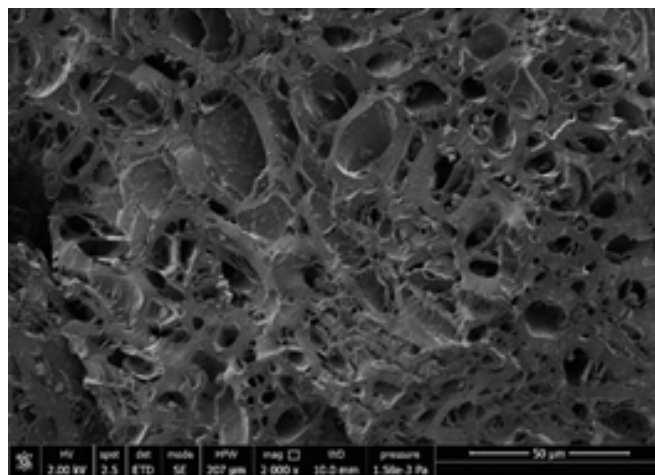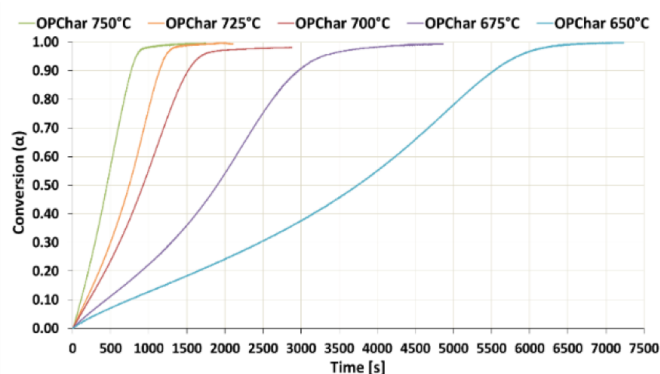

Fig. 4.   Char conversion as function of time at different temperatures at 50% steam and 50% N_2.

C. Integral Isoconversional Approach for Kinetic Parameters Determination

Fig. 5 shows the plot of lnt as function of T^{-1} obtained at different values of conversion. The results showed a good linearity (> 0.98), which indicates good reliability of results. Each line is representative of a specific conversion. In accordance with eq. 7, it follows that from the slop of the straight lines in Fig.5 it is possible to calculate the apparent activation energy at various degrees of conversion, in the range between 0.2 and 0.8.

Following the same approach, Fig. 6 shows lines obtained by plotting ln (t) as function of ln (P), Hence, the reaction order can be obtained from the slopes of the best fitting straight line, as indicated by eq. 9, showing also in this case a good linearity.

The apparent activation energies expressed as function of conversion is given in Fig. 7. The Ea values did not show significant variation with the conversion degree. The highest and the lowest activation energy values were obtained at 0.3 and 0.8 conversion degree, reaching 164 and 156 kJ/mol, respectively. The reaction order showed an almost constant trend with conversion, varying from 0.92 to 0.95 (see Fig.

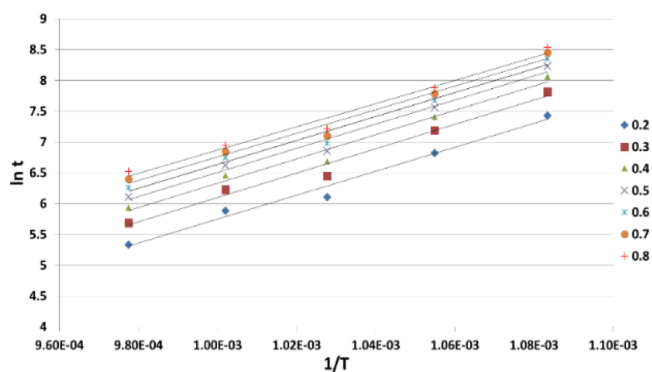| a	E	n	A
-	[kJ/mol]	-	[s^{-1}bar^{-n}]
0.2	161	0.95	5.06E+05
0.3	164	0.95	7.40E+05
0.4	163	0.95	7.10E+05
0.5	163	0.95	6.41E+05
0.6	161	0.94	5.30E+05
0.7	158	0.93	3.84E+05
0.8	156	0.92	2.95E+05

Fig. 5.   Plot of $ln(t_i)$ vs 1/T at different conversion.

8). This indicates that olive pomace char conversion in steam atmosphere is adsorption limited, and remains so since n is very close to one.

As mentioned in section 2, the pre-exponential factor was obtained through the application of the compensation effect. The results of the kinetic study for the determination of the kinetic triplets is shown in table IV. It can be observed that the
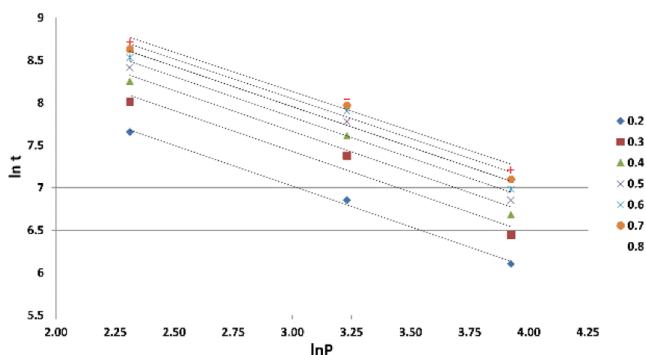

Fig. 6.   Plot of $ln(t_i)$ vs 1/T at different conversion.
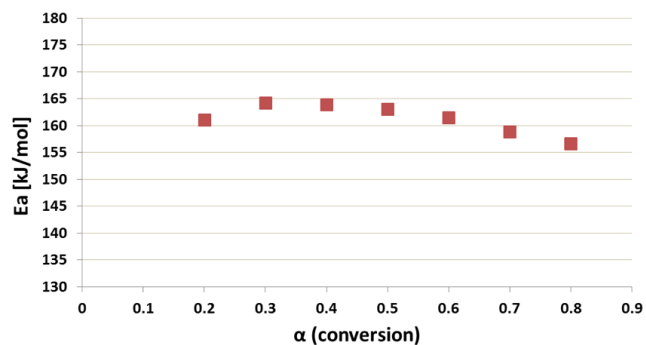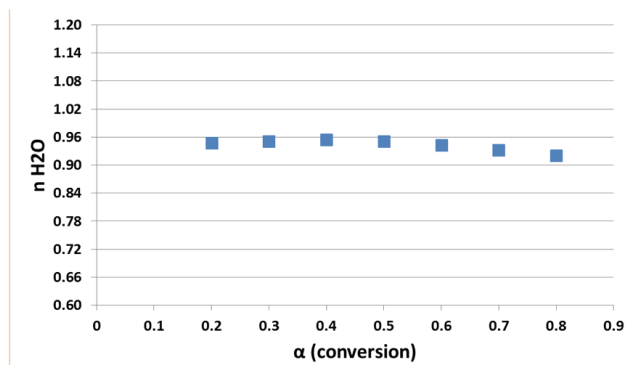

Fig. 7.   Activation energy as function of conversion.

Fig. 8.   Reaction order as function of conversion.

pre-exponential factor reach the maximum at $\alpha = 0.3$, equal to $7.4 * 10^5 s^{-1} bar^{-n}$, while the minimum was found at the end of process, resulting equal to $2.95 * 10^5 s^{-1} bar^{-n}$.

IV. CONCLUSIONS

Isothermal steam gasification experiments of chars obtained from the pyrolysis of dry olive pomace were conducted in a laboratory scale reactor. Ultimate and proximate analysis of the parent biomass were carried out. Furthermore, the metal composition and morphology of the char was studied. The specific surface area of olive pomace char before conversion was relative low, while it increased at 50% of conversion up to $500\,m^2/g$, involving the formation of a microstructure for the activation action of steam. This phenomenon is also followed by the formation of larger external pores, observed by means of SEM images.

The char showed a sigmoidal mode of conversion with time at each investigated temperature. The effect of temperature on time of conversion was relevant in the range 650-700° C, while from 700 to 750° C a slighter effect was observed. Apparent activation energy showed a slight variation with conversion, ranging from 156 to 164 kJ/mol. Similarly, the reaction order was almost constant, around the average value of 0.94.

ACKNOWLEDGMENT

for the support in the thermogravimetric analysis.

REFERENCES

[1] V. Chiodo, G. Zafarana, S. Maisano, S. Freni, A. Galvagno, and F. Urbani, "Molten carbonate fuel cell system fed with biofuels for electricity production," *International Journal of Hydrogen Energy*, vol. 41, no. 41, pp. 18 815–18 821, 2016.

[2] A. Galvagno, M. Prestipino, G. Zafarana, and V. Chiodo, "Analysis of an integrated agro-waste gasification and 120 kw sofc chp system: Modeling and experimental investigation," vol. 101, 2016, pp. 528–535.

[3] M. Prestipino, V. Palomba, S. Vasta, A. Freni, and A. Galvagno, "A simulation tool to evaluate the feasibility of a gasification-i.c.e. system to produce heat and power for industrial applications," vol. 101, 2016, pp. 1256–1263.

[4] W. Gadek, M. Mlonka-Mdrala, M. Prestipino, P. Evangelopoulos, S. Kalisz, and W. Yang, "Gasification and pyrolysis of different biomasses in lab scale system: A comparative study," vol. 10, 2016.

[5] G. Cannistraro, M. Cannistraro, A. Cannistraro, A. Galvagno, and G. Trovato, "Technical and economic evaluations about the integration of co-trigeneration systems in the dairy industry," *International Journal of Heat and Technology*, vol. 34, no. 2, pp. S332–S336, 2016.

[6] ——, "Reducing the demand of energy cooling in the ced, centers of processing data, with use of free-cooling systems," *International Journal of Heat and Technology*, vol. 34, no. 3, pp. 498–502, 2016.

[7] S. Brusca, A. Galvagno, R. Lanzafame, A. Marino Cugno Garrano, and M. Messina, "Performance analysis of biofuel fed gas turbine," vol. 81, 2015, pp. 493–504.

[8] G. Cannistraro, M. Cannistraro, A. Cannistraro, A. Galvagno, and G. Trovato, "Evaluation on the convenience of a citizen service district heating for residential use. a new scenario introduced by high efficiency energy systems," *International Journal of Heat and Technology*, vol. 33, no. 4, pp. 167–172, 2015.

[9] J. Popp, Z. Lakner, M. Harangi-Rkos, and M. Fri, "The effect of bioenergy expansion: Food, energy, and environment," *Renewable and Sustainable Energy Reviews*, vol. 32, pp. 559–578, 2014.

[10] S. Brusca, R. Lanzafame, A. Marino Cugno Garrano, and M. Messina, "Dynamic analysis of combustion turbine running on synthesis gas," *International Journal of Applied Engineering Research*, vol. 10, no. 21, pp. 42 244–42 253, 2015.

[11] S. Brusca, F. Famoso, R. Lanzafame, S. Mauro, M. Messina, and S. Strano, "Pm10dispersion modeling by means of cfd 3d and eulerian-lagrangian models: Analysis and comparison with experiments," vol. 101, 2016, pp. 329–336.

[12] M. Calì, D. Speranza, and M. Martorelli, "Dynamic spinnaker performance through digital photogrammetry, numerical analysis and experimental tests," in *Advances on Mechanics, Design Engineering and Manufacturing*. Springer, 2017, pp. 585–595.

[13] G. L. Sciuto, G. Susi, G. Cammarata, and G. Capizzi, "A spiking neural network-based model for anaerobic digestion process," in *2016 International Symposium on Power Electronics, Electrical Drives, Automation and Motion (SPEEDAM)*, June 2016, pp. 996–1003.

[14] S. Brusca, F. Famoso, R. Lanzafame, S. Mauro, A. Garrano, and P. Monforte, "Theoretical and experimental study of gaussian plume model in small scale system," vol. 101, 2016, pp. 58–65.

[15] S. Brusca, R. Lanzafame, and M. Messina, "Design and performance of a straight-bladed darrieus wind turbine," *International Journal of Applied Engineering Research*, vol. 10, no. 16, pp. 37 431–37 438, 2015.

[16] M. Calì, G. Sequenzia, S. M. Oliveri, and G. Fatuzzo, "Meshing angles evaluation of silent chain drive by numerical analysis and experimental test," *Meccanica*, vol. 51, no. 3, pp. 475–489, 2016.

[17] G. Capizzi, G. Lo Sciuto, M. Woźniak, and R. Damaševicius, *A Clustering Based System for Automated Oil Spill Detection by Satellite Remote Sensing*. Springer International Publishing, 2016, pp. 613–623.

[18] F. Famoso, R. Lanzafame, S. Maenza, and P. Scandura, "Performance comparison between micro-inverter and string-inverter photovoltaic systems," vol. 81, 2015, pp. 526–539.

[19] S. Brusca, R. Lanzafame, and M. Messina, "Wind turbine placement optimization by means of the monte carlo simulation method," *Modelling and Simulation in Engineering*, vol. 2014, 2014.

[20] E. Pedulla, F. L. Savio, G. Plotino, N. M. Grande, S. Rapisarda, G. Gambarini, and G. La Rosa, "Effect of cyclic torsional preloading on cyclic fatigue resistance of protaper next and mtwo nickel–titanium instruments," *Giornale Italiano di Endodonzia*, vol. 29, no. 1, pp. 3–8, 2015.

[21] G. La Rosa and F. Lo Savio, "A first approach to the experimental study of fracture parameters in opening and mixed mode by caustics," *Procedia Engineering*, vol. 109, pp. 418–426, 2015.

[22] G. La Rosa, C. Clienti, and F. L. Savio, "Fatigue analysis by acoustic emission and thermographic techniques," *Procedia Engineering*, vol. 74, pp. 261–268, 2014.

[23] C. Hognon, C. Dupont, M. Grateau, and F. Delrue, "Comparison of steam gasification reactivity of algal and lignocellulosic biomass: Influence of inorganic elements," *Bioresource Technology*, vol. 164, pp. 347–353, 2014.

[24] E. Gucciardi, V. Chiodo, S. Freni, S. Cavallaro, A. Galvagno, and J. Bart, "Ethanol and dimethyl ether steam reforming on rh/al2o 3 catalysts for high-temperature fuel-cell feeds," *Reaction Kinetics, Mechanisms and Catalysis*, vol. 104, no. 1, pp. 75–87, 2011.

[25] S. Vyazovkin, A. Burnham, J. Criado, L. Prez-Maqueda, C. Popescu, and N. Sbirrazzuoli, "Ictac kinetics committee recommendations for performing kinetic computations on thermal analysis data," *Thermochimica Acta*, vol. 520, no. 1-2, pp. 1–19, 2011.

[26] A. Caramagna, F. Famoso, R. Lanzafame, and P. Monforte, "Analysis of vertical profile of particulates dispersion in function of the aerodynamic diameter at a congested road in catania," vol. 82, 2015, pp. 702–707.

[27] S. Brusca, R. Lanzafame, and M. Messina, "Flow similitude laws applied to wind turbines through blade element momentum theory numerical codes," *International Journal of Energy and Environmental Engineering*, vol. 5, no. 4, pp. 313–322, 2014.

[28] ——, "Low-speed wind tunnel: Design and build," *Wind Tunnels: Aerodynamics, Models and Experiments*, pp. 189–220, 2011.

[29] S. Brusca, F. Famoso, R. Lanzafame, A. Marino Cugno Garrano, and P. Monforte, "Experimental analysis of a plume dispersion around obstacles," vol. 82, 2015, pp. 695–701.

[30] S. Brusca, A. Galvagno, R. Lanzafame, and M. Messina, "Hybrid vehicles performances analysis: Feed-forward dynamic approach," *SAE Technical Papers*, 2010.

[31] C. Di Blasi, "Combustion and gasification rates of lignocellulosic chars," *Progress in Energy and Combustion Science*, vol. 35, no. 2, pp. 121–140, 2009.

[32] W. B. Association., "Global biomass potential towards 2035," *WBA factsheet*, 2015.

[33] S. G. M. P. e. a. Capizzi, G., "Cascade feed forward neural network-based model for air pollutants evaluation of single monitoring stations in urban areas," *International Journal of Electronics and Telecommunications,*, vol. 61, no. 4, pp. 327–332, 2015.

[34] I. E. Agency., "Mobilizing sustainable bioenergy supply chains," *IEA Bioenergy ExCo*, 2015.

[35] N. Cerone, F. Zimbardi, L. Contuzzi, M. Prestipino, O. Carnevale, V. Valerio, and A. Villone, "Improved performances of updraft gasification at pilot plant by torrefaction pretreatment of wood," 2016.

[36] S. YAZOVKIN and A. Wight, "Wight, model-free and model fitting approaches to kinetic analysis of isothermal and non-isothermal data," *Thermochimica Acta*, vol. 340-341, pp. 53–68, 1999.

[37] F. Famoso, R. Lanzafame, S. Maenza, and P. Scandura, "Performance comparison between low concentration photovoltaic and fixed angle pv systems," vol. 81, 2015, pp. 516–525.

[38] S. Brusca, R. Lanzafame, A. Marino Cugno Garrano, and M. Messina, "On the possibility to run an internal combustion engine on acetylene and alcohol," vol. 45, 2014, pp. 889–898.